Journal of Cereal Science 69 (2016) 321–328

Contents lists available at ScienceDirect

Journal of Cereal Science

journal homepage: www.elsevier.com/locate/jcs

# A high-throughput X-ray micro-computed tomography (μCT) approach for measuring single kernel maize (*Zea mays* L.) volumes and densities

Anina Guelpa [a], Anton du Plessis [b], Marena Manley [a, *]

[a] Department of Food Science, Stellenbosch University, Private Bag X1, Matieland, Stellenbosch, 7602, South Africa
[b] CT Scanner, Central Analytical Facilities, Stellenbosch University, Private Bag X1, Matieland, Stellenbosch, 7602, South Africa

ARTICLE INFO

*Article history:*
Received 17 November 2015
Received in revised form
18 April 2016
Accepted 19 April 2016
Available online 21 April 2016

*Keywords:*
*Zea mays* L.
X-ray micro-computed tomography
Maize milling quality
Kernel volume
Kernel density
Low resolution scans

ABSTRACT

Maize (*Zea mays* L.) meal, which is industrially produced using dry-milling, is an important staple food in many developing countries. Kernel hardness is often the characteristic that is measured to select hybrids desirable for milling. Conventional hardness methods present challenges and limitations. Therefore, high-throughput methodology was developed, using X-ray micro-computed tomography (μCT), to determine whole maize kernel volumes and densities as a means to discriminate between good and poor milling quality. Volume and density measurements of 150 kernels were obtained simultaneously from low-resolution (80 μm) μCT scans, reducing acquisition time and cost. Volume measurements were obtained for the individual kernels, as well as regions-of-interest (ROIs), i.e. vitreous and floury endosperm. Densities were also calculated for each maize kernel, as well as the ROIs, using a pre-developed density calibration. Classification results (77–93% correct classification), as obtained using descriptive statistics, i.e. receiver operating characteristic (ROC) curves, demonstrated X-ray μCT derived volume and density measurements of individual maize kernels as potential indicators of milling quality.

© 2016 Elsevier Ltd. All rights reserved.

## 1. Introduction

Maize (*Zea mays* L.) is a staple food source and apart from being consumed as fresh, boiled or roasted (maize ears), it can also be processed for the production of speciality foods (e.g. tortillas and tortilla chips) (Lee et al., 2012), or it can be shelled and milled to produce maize meal or semolina (Mestres et al., 1991). Maize is commercially milled using the dry-milling process. This process entails the removal of the germ and pericarp during a de-germing process (Serna-Saldivar, 2010), consequently exposing the endosperm that is further subjected to grinding and sieving (Watson, 1987). A high yield of pure endosperm fractions (Chiremba et al., 2011) with a low percentage chop (combination of pericarp, germ and to a lesser extent endosperm) is desirable. Percentage chop (% chop), a good indicator of milling quality, has been shown to correlate with hectoliter mass ($r = -0.71$) (Guelpa et al., 2015a). Hectolitre mass, in turn, is a measure of maize density (Dorsey-Redding et al., 1991) and determined as the weight of a known volume of grain. Maize kernel density is typically defined by the endosperm structure and more specifically the ratio of the two endosperm types (Delcour and Hoseney, 2010). Although these two endosperm types, i.e. vitreous and floury, comprise of similar starch tissue (Paiva et al., 1991), the starch granules in the vitreous endosperm are covered with a thick, continuous protein matrix, whereas this matrix is thin or absent in the floury endosperm (Watson, 1987). Accordingly, the starch granules of the harder and transparent vitreous endosperm are polygonally shaped and tightly packed, while the granules of the softer and opaque floury endosperm are loosely packed and round (Paiva et al., 1991; Watson, 1987). The densities of these two types of endosperms thus differ. Maize kernel density, as an indication of milling quality, can thus be expressed as the vitreous-to-floury endosperm (V:F) ratio (Delcour and Hoseney, 2010; Guelpa et al., 2015a, 2015b).

Numerous studies investigated the V:F ratio as a descriptor of as well as means to determine maize kernel hardness, mostly using tedious and time-consuming hand-dissection (Dombrink-Kurtzman, 1994; Gaytán-Martínez et al., 2006; Paulsen and Hill, 1985; Pomeranz et al., 1984; Robutti, 1995). A few studies used non-destructive methods (Erasmus and Taylor, 2004; Mestres et al.,

* Corresponding author.
*E-mail addresses:* aninag@sun.ac.za (A. Guelpa), anton2@sun.ac.za (A. du Plessis), mman@sun.ac.za (M. Manley).

http://dx.doi.org/10.1016/j.jcs.2016.04.009
0733-5210/© 2016 Elsevier Ltd. All rights reserved.

1991). Erasmus and Taylor (2004) developed a maize translucency detection instrument, whereas Mestres et al. (1991) calculated percentage vitreousness by measuring the respective areas from an enhanced photograph. Near infrared (NIR) hyperspectral imaging has also been used to quantify the respective endosperm types (McGoverin and Manley, 2012), non-destructively.

A great number of conventional hardness methods exist, significantly differing in approach and interpretation, and along with the absence of a standardised method, the measurement of maize hardness poses real challenges (Fox and Manley, 2009). It has, e.g. been demonstrated that when floating test densities (as an indication of kernel hardness) of the same kernels were compared to densities calculated with X-ray μCT data, misleading results were obtained (Guelpa et al., 2015b). The floating test consistently produced lower densities and a large bias was apparent. An advantage of X-ray μCT, i.e. allowing the exclusion of cavities, makes this method more suited for accurate density measurements (Guelpa et al., 2015b; Gustin et al., 2013). Although large cavities, usually visible close to the germ, could contribute to fractures during milling, it should not be included when measuring material density (Guelpa et al., 2015b) such as that of the floury or vitreous endosperm. Furthermore, due to the confirmed relationship between hectolitre mass and %chop, milling quality can thus also be expressed in terms of material (endosperm) density (Guelpa et al., 2015a).

Gustin et al. (2013) recognised the potential of X-ray μCT as a method to determine maize kernel volume and density. They also demonstrated that single kernel density correlated ($r = 0.8$) with hectolitre mass (Gustin et al., 2013), a conventional method of describing maize hardness (Lee et al., 2006). It was also shown how X-ray μCT could estimate maize hardness using a density calibration (Guelpa et al., 2015b). Threshold values, resulting from receiver operating characteristic (ROC) curves, were determined for whole kernel, and vitreous and floury endosperm densities, respectively which allowed for hardness classification (Guelpa et al., 2015b). These densities were calculated, using X-ray μCT scans of individual kernels, acquired at a high resolution of 13.4 μm. Furthermore, Takhar et al. (2011) indicated that experimental drying profiles could be predicted with reasonable accuracy and De Carvalho et al. (1999) studied stress cracks formation in maize kernels, caused by high temperatures or excess moisture. Both groups found the technique of X-ray μCT successful for maize kernel characterisation.

As X-ray μCT is an expensive method and X-ray acquisition a timely process, a high-throughput X-ray μCT approach is proposed in this study, scanning multiple (150) maize kernels simultaneously; although reducing the resolution of the scans. Two examples of high-throughput X-ray based methods include the use of low resolution CT scanning, to measure the relative wood densities from *Picea abies* wood cores (Steffenrem et al., 2014) and to determine the number of rice tillers on individual rice plants (Yang et al., 2011, 2013). The wood, as well as rice tillers studies used conventional X-ray CT systems in combination with industrial conveyors, also allowing automated extraction of relevant information (densities and the number of rice tillers per plant). These studies provided three advantages, i.e. absence of human disturbance, automation and high-throughput.

This work proposes novel methodology using X-ray μCT to measure whole kernel volumes and densities, as well as that of two respective regions-of-interest (ROIs), i.e. vitreous and floury endosperm, for the purpose to classify maize into milling quality classes. This method was designed to facilitate high-throughput X-ray acquisition of multiple maize kernels, simultaneously. It had to be established whether the X-ray μCT derived volume and density measurements calculated from lower resolution scans could still be used to classify maize kernels based on their milling quality (endosperm density), thereby making this method more cost-effective and less time-consuming.

## 2. Materials and methods

### 2.1. Samples

Forty-nine different white maize hybrids from South African breeding trails were kindly supplied by PANNAR Seeds (Greytown, South Africa) and included samples obtained from four localities (Greytown, Delmas, Klerksdorp and Schweizer-Reneke) and three plantings (early, normal or late) of the 2012 harvest season. The milling quality of the samples were determined according to their milling performance as measured during the actual milling process, although on pilot plant-scale. Good milling quality is indicated by a small percentage of hominy chop. Hominy chop (comprising the pericarp, tip cap, germ and some endosperm) is of lesser value than maize meal and grits and predominantly used as animal feed. Maize that mill poorly delivers a larger percentage chop (%chop) as soft endosperm is also included into the chop. Percentage chop is therefore used as an indication of the milling quality of maize, although it is not a recognised hardness measurement method as such. Subsequently, 20 of the hybrids were selected with 10 hybrids representing good and 10 poor milling quality. From each hybrid 15 kernels were randomly selected to be subjected to X-ray μCT scanning. Consequently, 150 maize kernels represented good, and 150 poor milling performance.

### 2.2. Sample preparation

Thirty maize kernels were randomly placed in each of 10 florist oasis discs (10 cm in diameter; 2 cm in height) to facilitate simultaneous X-ray μCT acquisition. The low density of the florist oasis provided for clear distinction from the subjects of interest and was therefore a suitable medium for mounting purposes. For optimal segregation, it was important that none of the kernels overlap or touched each other. Five florist oasis discs were stacked on top of each other and secured with a wooden stick to prevent any movement during the scanning process. For the construction of linear equations to develop the density calibrations, 7 polymer discs of known but different densities were obtained. The densities of the polymer discs covered that of typical maize kernels. These 7 polymer discs (25 mm in diameter and 10 mm in height), comprising polytetrafluoroethylene (PTFE) (2.15 g $cm^{-3}$); sustanat polycarbonate (PC) (1.2 g $cm^{-3}$); ultra-high molecular weight polyethylene (UHMW PE) (0.92 g $cm^{-3}$); polypropylene (PP) (0.91 g $cm^{-3}$); high density polyethylene (HDPE) (0.91 g $cm^{-3}$); polyethylene terephthalate (PET) (1.38 g $cm^{-3}$); and sustarin C acetal/nylon (1.15 g $cm^{-3}$), were also placed in each florist oasis stack to facilitate the construction of the linear equations (density calibration function) (Du Plessis et al., 2013; Guelpa et al., 2015b).

### 2.3. X-ray μCT image acquisition

X-ray scans were acquired using a commercial micro-focus X-ray computed tomography system, i.e. Phoenix V|Tome|X L240 (General Electric Sensing and Inspection Technologies/Phoenix X-ray, Wunstorff, Germany). The system is located at the CT Scanner Facility of the Central Analytical Facility (CAF), Stellenbosch University, South Africa. It comprises a lead-lined cabinet that houses the X-ray direct tube and the sample manipulator, along with a cooling unit and an external control module. Image acquisition was set at 500 ms per image with 2000 images recorded in one rotation at 80 μm voxel size or resolution. A 0.1 mm copper filter was used to reduce beam hardening artefacts and a scan took 1 h to complete. In

this work a tungsten target, 60 kV and 240 μA was used for X-ray generation.

Five of the florist oasis stacks, containing 150 maize kernels in total, were selected and placed on the specimen stage and rotated along the axis, perpendicular to the beam direction. Two scans were thus required to image all 300 kernels.

### 2.4. X-ray μCT image processing and analysis

The acquired 2D X-ray images were rendered into 3D volumes, using the integrated Phoenix Datos acquisition and reconstruction software (General Electric Sensing and Inspection Technologies/ Phoenix X-ray, Wunstorff, Germany). Reconstruction comprises filtered back-projection algorithms where the grey values in a rendered CT image represent the attenuation in each pixel (Singhal et al., 2013) (Fig. 1a). The 3D images were further analysed with VGStudio Max 2.2 software (Volume Graphics, Heidelberg, Germany). Each maize kernel was analysed independently as sub volume extraction was possible. Volume analysis, as well as density calculations, were performed per kernel.

### 2.5. Volume analysis

Entire kernel volume (EKV) and the volumes of the two endosperm types, i.e. vitreous (VEV) and floury endosperm (FEV), was determined using the automated Region growing tool, in combination with the Volume analyser function of VGStudio Max 2.2. In order to quantify the respective endosperm types, separation had to be established that was only possible with the exclusion of the germ region (Guelpa et al., 2015b). The endosperm type volumes (VEV and FEV) were expressed as a percentage of the total volume of endosperm per kernel. Additionally, a vitreous-to-floury endosperm ratio (V:F) was calculated from the VEV and FEV.

### 2.6. Construction of calibration function and density calculations of individual maize kernels

Densities of entire maize kernels (EKD), as well as two regions of interest (ROIs), i.e. the vitreous (VED) and floury endosperm (FED), were calculated using a density calibration function as described in Guelpa et al. (2015b). Constructing the calibration function required the average grey value of a representative volume from each polymer disc. Each voxel has an associated grey value depending on the polymers' density and atomic number. The average grey values of the polymer discs were therefore measures of their densities and subsequently used to generate the two density calibration functions according to Equation (1). The calibration functions were subsequently used for the calculation of the densities of the two groups of 150 individual maize kernels, respectively.

$$\text{Density (g cm}^{-3}) = \mathbf{m} \times \text{grey value} + \mathbf{c} \quad (1)$$

where **m** is the slope and **c** is the intercept. The grey value in the equation was substituted with the average grey value of the ROI, e.g. entire kernel, vitreous or floury endosperm. Since maize endosperm texture (density) is typically defined as the ratio between the vitreous and floury (V:F) endosperm (Delcour and Hoseney, 2010), the density measurements were determined as material density. Intergranular air pockets or pores, typically present as small air spaces (with volumes smaller than 1 voxel (80 μm)) in the endosperm were included in the density measurements. However, large cavities or large air spaces, usually present around the germ, that could not be associated with either of the two endosperm types were not included in the material density measurements.

It was noticed that the densities of the germ and vitreous endosperm regions were similar and thus prevented accurate

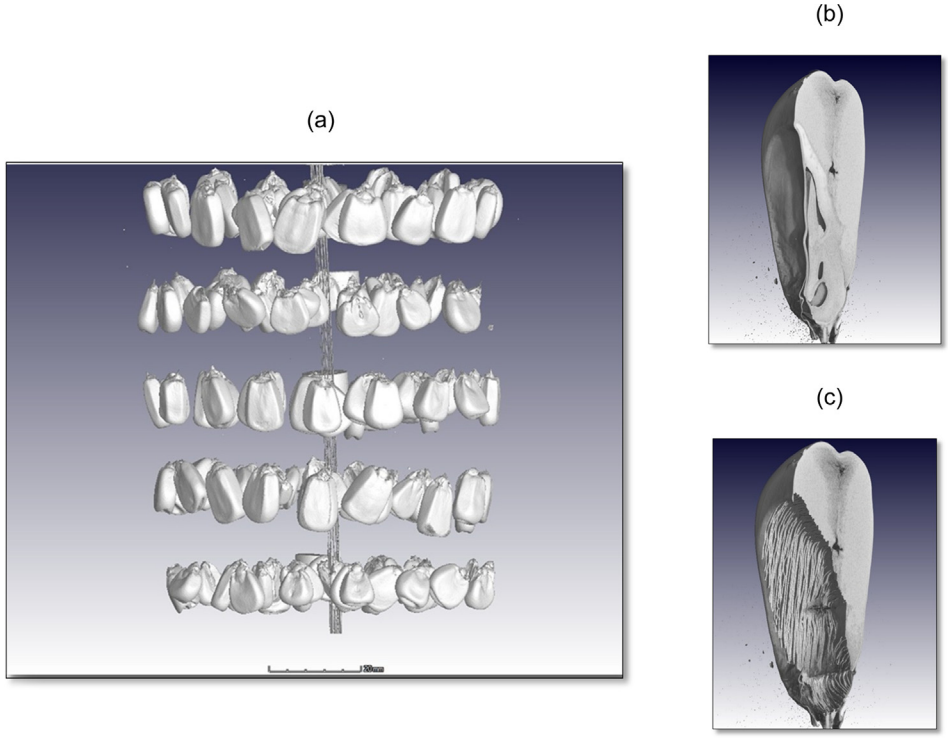


**Fig. 1.** 3D X-ray μCT images of (a) the stack of five discs, each containing 30 kernels, with the mounting material removed, revealing the 150 maize kernels; (b) a maize kernel with the germ intact, and (c) germ removed.

separation of the two endosperm types. Therefore, the germ region was removed, slice by slice, for each kernel using the drawing tool (Guelpa et al., 2015b) as illustrated in Fig. 1b and c. After this 'virtual' removal of the germ, the remaining endosperm could be separated into vitreous and floury regions, respectively, and mean grey values for the ROIs could be obtained. The grey values were substituted into the calibration equations (one for each X-ray scan) and subsequent densities of each individual kernel were calculated as described by Guelpa et al. (2015b) and expressed as g $cm^{-3}$.

### 2.7. Validating the accuracy of X-ray μCT density calculations

The accuracy of the μCT density measurements was tested by comparing the estimated (μCT) kernel mass with the measured (weighted) mass (Gustin et al., 2013; Guelpa et al., 2015b). The estimated kernel mass was calculated by multiplying the EKV with the EKD (both derived from μCT), using the mathematical relationship between mass, volume and density. Subsequently, he mass of each of 300 kernels were weighed using a laboratory scale (Precisa, Instrulab, Johannesburg, South Africa), accurate to three decimals.

### 2.8. Statistical analysis

#### 2.8.1. Univariate

Mean differences for the X-ray μCT derived variables (densities: EKD, VED and FED, and volumes: EKV, VEV and FEV, also V:F) were evaluated by one-way analysis of variance (ANOVA) using STATISTICA version 11 (StatSoft, Inc., Tulsa, USA).

Furthermore, receiver operating characteristic (ROC) curves were determined with STATISTICA as descriptive statistics to demonstrated the ability of volume and density measurements of individual maize kernels to be used as potential indicators of milling quality (good and poor milling quality). The variables used were as obtained from X-ray μCT derived measurements (EKV, VEV, FEV, EKD, VED, FED and V:F). A ROC curve is a plot of sensitivity (or true positive rate) on the y-axis against 1-specificity (or true negative rate) on the x-axis, for varying values of the threshold. This results in a graphical plot that illustrates the performance of a binary classifier system as its discrimination threshold is varied. The optimal threshold is determined by maximising the sum of sensitivity and specificity. The calculated area under the ROC curve is a measure of the classification accuracy achieved and expressed as a percentage.

Spearman's rank correlation coefficients were used to test the strength of the relationships between pairs of X-ray μCT derived results (densities: EKD, VED and FED, and volumes: EKV, VEV and FEV, also V:F) using STATISTICA.

To assess the accuracy of the μCT density measurements, estimated (μCT) kernel masses were compared to measured (weighed) masses, and the interclass correlation (ICC) coefficients were subsequently determined. The ICC agreement correlates measurements with each other, while taking into account the differences in absolute values of the respective measurements, and the ICC consistency only correlates measurements. All ICC calculations were done in R statistical programming language (R Package Concord).

#### 2.8.2. Multivariate: principal component analysis

Principal component analysis (PCA) was performed on X-ray μCT derived variables (densities: EKD, VED and FED, and volumes: EKV, VEV and FEV, also V:F). To inspect the relationship between the variables, PCA bi-plots were used as it combines the scores and the loadings. STATISTICA was used to perform the PCA.

## 3. Results and discussion

### 3.1. X-ray μCT volume analysis

X-ray μCT allowed the quantification of the following volumes: EKV, VEV and FEV, based on grey value thresholding of the respective ROIs. EKV included the volume inside the contour lines drawn around the entire kernel, after removal of cavities. To segment VEV and FEV, the germ region had to be excluded using the drawing tool. Thereafter, a higher grey value threshold was applied to select the vitreous endosperm region, while excluding the floury endosperm region. A region growing tool identified voxels belonging to the selected grey value intervals and quantified the volumes, using a volume analyser tool. Floury endosperm was quantified using the same method, although a lower grey value interval had to be selected for segmentation.

Due to artifacts affecting three of the imaged maize kernels, these kernels could not be used for image analysis. Consequently, only 297 samples were used throughout this study. Mean volumes for the entire sample set (n = 297) were: 251.64 $mm^3$, 161.85 $mm^3$ and 90.28 $mm^3$ for EKV, VEV and FEV, respectively.

The mean EKV of the good milling hybrids was significantly ($P < 0.01$) larger (321.50 $mm^3$) than that of the poor milling hybrids (255.56 $mm^3$) (Table 1). Also the mean VEV for the good milling hybrids (199.70 $mm^3$) was significantly ($P < 0.01$) larger than that of the poor milling hybrids (123.23 $mm^3$), whereas the mean FEV for the good milling hybrids (78.88 $mm^3$) was significantly ($P < 0.01$) smaller than that of the poor milling hybrids (101.91 $mm^3$). These results agreed with the higher proportion of vitreous endosperm found in good milling kernels (Weber et al., 2014). Similar results were obtained when Erasmus and Taylor (2004), after analysing 245 white maize kernels specifically bred for milling purposes using image analysis, found the endosperm percentages to vary between 46.3% and 63.7% (dry mass of vitreous endosperm divided by dry mass of whole kernel).

The V:F results obtained indicated a significantly ($P < 0.01$) higher V:F for the good milling (2.77) compared to that of the poor milling kernels (1.27) (Table 1). A similar trend was observed in the study by McGoverin and Manley (2012) who quantified vitreous and floury endosperm proportions within maize kernels by developing a NIR hyperspectral imaging classification model (V:F = 4.9 for hard (good milling) kernels, and 2.6 for soft (poor milling) kernels, respectively).

Although the acquisition of numerous kernels in one scan resulted in lowering the resolution (80 μm) of the scans, efficient segmentation and quantification could still be achieved and the results were comparable to those of a former study done at a higher resolution (13.4 μm) (Guelpa et al., 2015b).

### 3.2. X-ray μCT density calculations

Due to the images obtained with two scans, 150 kernels per scan, two linear equations had to be constructed (Equations (2) and (3)) to enable density calculations.

$$\text{Density (g cm}^{-3}) = 3.6 \times 10^{-5} \times \text{grey value} - 0.1100 \ (R^2 = 0.997) \quad (2)$$

$$\text{Density (g cm}^{-3}) = 3.5 \times 10^{-5} \times \text{grey value} - 0.0659 \ (R^2 = 0.997) \quad (3)$$

The average EKD of all 297 maize kernels were 1.30 g $cm^{-3}$, while that of the VED and FED were 1.36 g $cm^{-3}$ and 1.12 g $cm^{-3}$, respectively (Table 1). Mean EKD of the good milling hybrids (1.31 g $cm^{-3}$) was significantly ($P < 0.05$) higher than that of the poor milling hybrids (1.23 g $cm^{-3}$) as expected with the higher

**Table 1**
Volume and density results as derived by X-ray μCT for the two milling classes, good (n = 150) and poor (n = 147), also indicating ANOVA results.

| | Good milling hybrids | | Poor milling hybrids | | *P*-value |
|---|---|---|---|---|---|
| | Range | Mean ± SD | Range | Mean ± SD | |
| EKV ($mm^3$) | 158.4–447.7 | 321.5 ± 51.4 | 143.1–444.0 | 255.6 ± 70.1 | <0.01 |
| VEV ($mm^3$) | 66.4–313.7 | 199.7 ± 39.7 | 35.9–282.8 | 123.2 ± 51.8 | <0.01 |
| FEV ($mm^3$) | 34.5–188.4 | 78.9 ± 23.5 | 52.0–218.1 | 101.9 ± 26.7 | <0.01 |
| V:F | 0.69–7.18 | 2.77 ± 1.04 | 0.2–3.71 | 1.27 ± 0.58 | <0.01 |
| EKD (g $cm^{-3}$) | 1.22–1.36 | 1.31 ± 0.03 | 0.97–1.32 | 1.23 ± 0.05 | <0.01 |
| VED (g $cm^{-3}$) | 1.26–1.42 | 1.38 ± 0.03 | 1.23–1.40 | 1.35 ± 0.03 | <0.01 |
| FED (g $cm^{-3}$) | 1.04–1.26 | 1.14 ± 0.04 | 0.89–1.27 | 1.10 ± 0.04 | <0.01 |

SD: Standard deviation.
EKV: Entire kernel volume.
VEV: Vitreous endosperm volume.
FEV: Floury endosperm volume.
V:F: Vitreous-to-floury endosperm ratio.
EKD: Entire kernel density.
VED: Vitreous endosperm density.
FED: Floury endosperm density.

proportion of vitreous endosperm present within good milling (or hard) hybrids (Watson, 1987), which would increase the density. The protein matrix within this endosperm type keeps the starch granules tightly packed, thus dense, as opposed to more intracellular air spaces found within the loosely packed floury endosperm (Robutti et al., 1997). The same trend was found for the mean VED and FED, as these values were also significantly higher for the good milling hybrids (1.38 g $cm^{-3}$ and 1.14 g $cm^{-3}$, respectively) compared to the poor milling hybrids (1.35 g $cm^{-3}$ and 1.10 g $cm^{-3}$, respectively) (Table 1).

The density results of the lower resolution scans were compared to those of the higher resolution scans, as reported by Guelpa et al. (2015b). At 13.4 μm resolution, the average EKD of 16 maize kernels were 1.49 g $cm^{-3}$, while that of the VED and FED were 1.67 g $cm^{-3}$ and 1.34 g $cm^{-3}$, respectively. All these density measurements were higher than those obtained in the lower resolution study. It should, however, be stressed that the hybrids used in the higher resolution study were selected based on milling performance results using the particle size index (PSI) method. Clearly, in the higher resolution study, overall higher density kernels were used. For the current study, hybrids selection took place based on %chop results.

The proposed method could indeed be used for cost-efficient and high-throughput measurements of maize densities, i.e. EKD, VED and FED, on low resolution data of 80 μm from a large number of maize kernels scanned at once. When comparing speed of data processing, the higher resolution (13.4 μm) data accumulation of 16 individual kernels required 3.5 h (Guelpa et al., 2015b). The high-throughput method reported in this paper allowed the same results to be obtained in approximately 16 h for all 300 kernels, i.e. if directly compared 3 min (low resolution) vs. 13 min (high resolution). The lower resolution scans thus simplified data processing and analysis. Also, the virtual removal of the germ was less time-consuming due to fewer 2D image slices being present in the low resolution images. Selection of ROI requires manual selection of each slice, in this case the germ. Although the higher resolution scans enabled quantification of microstructural properties such as porosity (Guelpa et al., 2015b), not possible at the lower resolution, it is not required to determine maize endosperm densities (EKD, VED and FED) that could be used for classification purposes. Similarly, scans acquired at 3 μm resolution, using a Nanotom S μCT system, revealed very clearly the porosity within a maize kernel (Guelpa et al., 2015b), but not essential for efficient classification based on endosperm density.

The greatest benefit of this X-ray μCT approach, compared to conventional hardness methods using density measurements, is the ability to measure true densities not including cavities. Maize milling quality is related to the ratio in which the vitreous and floury endosperm is present in kernels, and this functionality of X-ray CT to select only the desirable ROIs was illustrated in this method.

### 3.3. Validation of the accuracy of the X-ray μCT density calibration

The accuracy of this high-throughput μCT density calibration was tested by comparing the calculated μCT kernel masses (hereby referred to as the estimated masses) with measured (weighed) masses (hereby referred to as the actual masses) (Guelpa et al., 2015b). The estimated masses ranged from 0.133 to 0.557 g

**Table 2**
Receiver operating characteristic (ROC) curve classification results when using X-ray μCT volumes and densities as variables.

| | Sensitivity (%) | Specificity (%) | Threshold | Area under curve (%) |
|---|---|---|---|---|
| EKV ($mm^3$) | 79 | 68 | 251.60 | 75 |
| VEV ($mm^3$) | 81 | 82 | 176.14 | 87 |
| FEV ($mm^3$) | 78 | 67 | 84.3 | 77 |
| V:F | 85 | 90 | 1.99 | 92 |
| EKD (g $cm^{-3}$) | 85 | 88 | 1.28 | 93 |
| VED (g $cm^{-3}$) | 68 | 77 | 1.37 | 79 |
| FED (g $cm^{-3}$) | 71 | 74 | 1.12 | 78 |

EKV: Entire kernel volume.
VEV: Vitreous endosperm volume.
FEV: Floury endosperm volume.
V:F: Vitreous-to-floury endosperm ratio.
EKD: Entire kernel density.
VED: Vitreous endosperm density.
FED: Floury endosperm density.

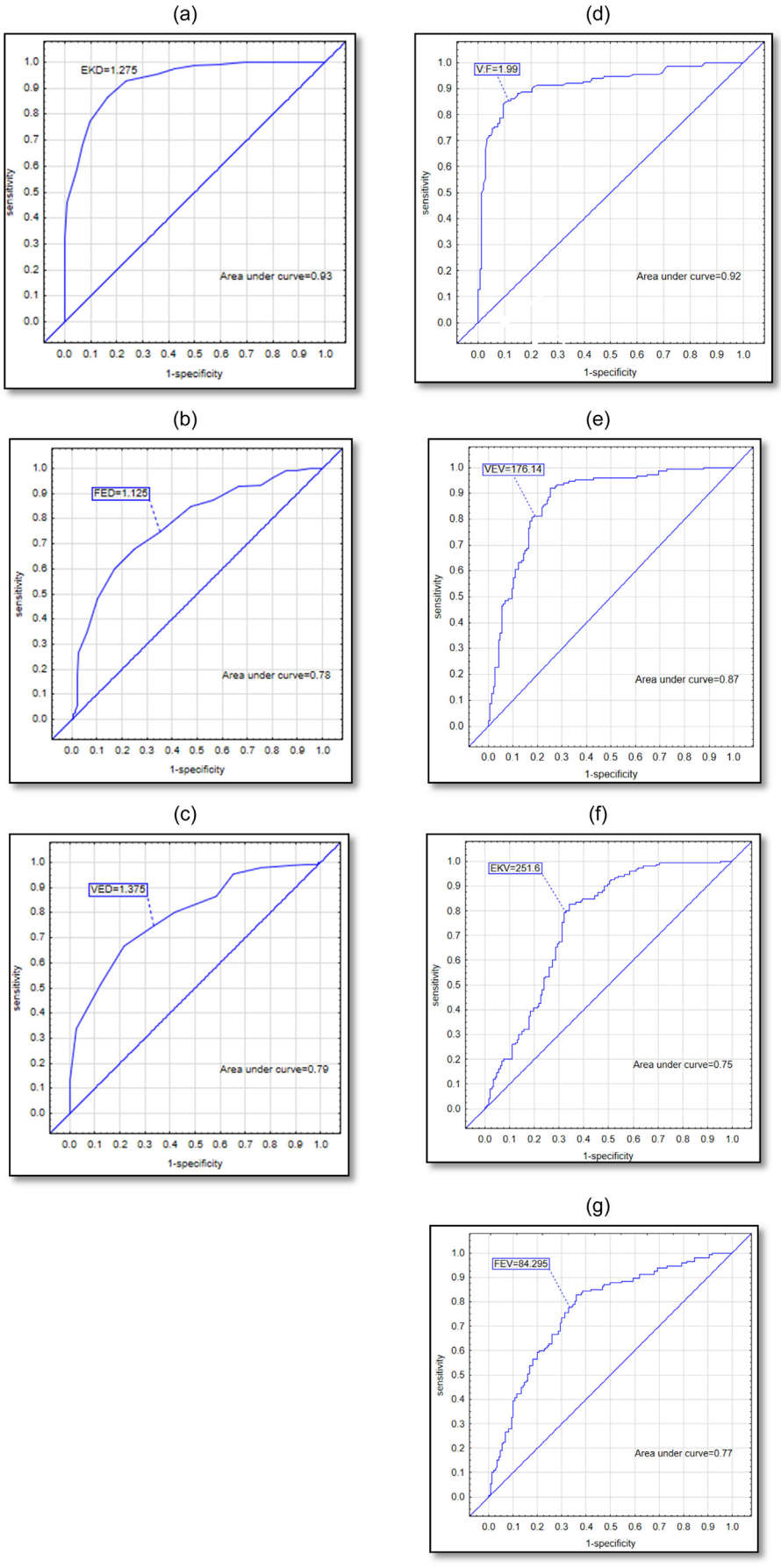


**Fig. 2.** Receiver operating characteristic (ROC) curves indicating milling quality classification using (a) entire kernel density (EKD); (b) vitreous endosperm density (VED); (c) floury endosperm density (FED); (d) vitreous-to-floury endosperm ratio (V:F); (e) vitreous endosperm volume (VEV); (f) entire kernel volume (EKV); and (g) floury endosperm volume (FEV) as derived by X-ray μCT.

(mean ± SD; 0.321 ± 0.082 g) with the actual masses ranging from 0.159 to 0.649 g (mean ± SD; 0.383 ± 0.100 g). The high ICC consistency of 0.84 confirmed that the results of the two methods were comparable, which was also indicated by a correlation coefficient of 0.86 (Spearman rank coefficient). However, a lower ICC agreement of 0.69 indicated that a bias was present, which was evident in the estimated masses being constantly lower than that of the measured masses. A decrease in accuracy was apparent in this study, compared to a former study done at a higher resolution, as no bias was found (ICC consistency = 0.99; ICC agreement = 0.96), along with a lower standard error of measurement (0.010 g compared to 0.037 g).

### 3.4. Milling classification

The kernels were subjected to a classification method, i.e. ROC curves (Table 2). When using ROC curves, a threshold value is obtained after optimising the sum of the sensitivity (x-axis) and the specificity (y-axis), which indicates the cut-off point for a sample to belong to a respective class. Good classifications in terms of milling quality were obtained for all the X-ray μCT derived variables, with the highest classification accuracy obtained for EKD (Fig. 2a) (area under curve = 93%). A threshold value of 1.28 g $cm^{-3}$ classified kernels with higher densities as good milling hybrids and with densities lower as the threshold value as poor milling hybrids (Table 2). This indicated that the lower resolution data captured sufficient detail in order to achieve good classification accuracies when considering whole kernel densities. Classification using the other two density variables, i.e. VED (Fig. 2c) and FED (Fig. 2b), resulted in reasonably good classifications (area under curve = 79% and 78%, respectively). The feasibility of this study was therefore best demonstrated with the use of EKD for classification purposes. This variable (EKD) was also easier to calculate than that of the respective ROIs (VED and FED) as no additional data analysis (in the form of removing the germ region) was needed. The classification results obtained were acceptable, although, weaker than those obtained by a similar study performed at higher resolution (100% correct classification for all the density measurements, i.e. EKD, VED and FED) (Guelpa et al., 2015b).

Classifications achieved when using volume measurements, were also good. A classification accuracy of 87% was obtained for VEV (Fig. 2e), whereas slightly poorer classification accuracies were obtained for EKV (75%) and FEV (77%) (Fig. 2f and g). A decent classification accuracy of 92% was achieved for V:F (Fig. 2d). This is in accordance with the consideration that the ratio of vitreous-to-floury endosperm dictates the milling quality thereof (Robutti, 1995). Therefore, in order to classify single maize kernels into milling quality classes, the use of V:F as derived from X-ray μCT scans of low resolution data is also a feasible possibility.

### 3.5. Principal component analysis (PCA) of the X-ray μCT derived variables

The interaction of all the variables (volumes and densities) of the entire sample set was illustrated in the PCA bi-plot (Fig. 3). All these measurements were done on individual kernels (n = 297). The first two principal components (PCs) explained 76% of the variation within the model, with PC 1 explaining the most (56%). Milling quality was described in the direction of PC 1. This was in accordance with the hardness (hard and soft kernels) study of Guelpa et al. (2015b).

The loadings indicated the relationship between the variables, and in particular, it could be observed that a stronger correlation existed between V:F, EKD, VEV, VED, FED and EKV. FEV showed no correlation. Considering the Spearman's rank correlation coefficients (Table 3), it was apparent that FEV was indeed poorly correlated with the other variables, except with V:F (r = −0.70, $P < 0.01$). Although FEV showed a poor relationship with the other variables in the PCA bi-plot, a good classification accuracy of 77% was obtained (using ROC curves) when classifying good and poor milling kernels based on this measurement.

The strongest correlations were indicated to be that of VEV and EKV (r = 0.89, $P < 0.01$) and VEV and V:F (r = 0.85, $P < 0.01$). The

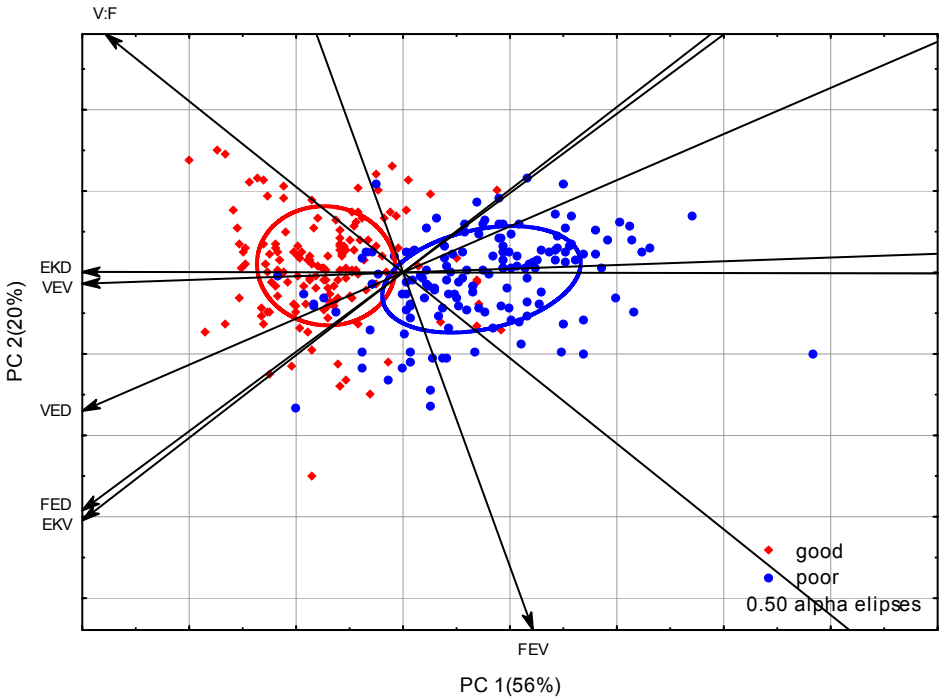


**Fig. 3.** Principal component analysis (PCA) bi-plot (PC 1 vs. PC 2), illustrating the interaction between the X-ray μCT derived variables from 297 maize kernels.

**Table 3**
Spearman's rank correlation coefficient matrix for the X-ray μCT variables performed on individual maize kernels (n = 297).

| | EKV | VEV | FEV | V:F | EKD | VED | FED |
|---|---|---|---|---|---|---|---|
| EKV | 1.00 | | | | | | |
| VEV | 0.89* | 1.00 | | | | | |
| FEV | 0.20* | −0.26* | 1.00 | | | | |
| V:F | 0.53* | 0.85* | −0.70* | 1.00 | | | |
| EKD | 0.27* | 0.76* | −0.45* | 0.77* | 1.00 | | |
| VED | 0.31* | 0.39* | −0.16* | 0.36* | 0.80* | 1.00 | |
| FED | 0.17** | 0.39* | −0.04*** | 0.30* | 0.76* | 0.64* | 1.00 |

EKV: Entire kernel volume ($mm^3$).
VEV: Vitreous endosperm volume ($mm^3$).
FEV: Floury endosperm volume ($mm^3$).
V:F: Vitreous-to-floury endosperm ratio.
EKD: Entire kernel density ($g\ cm^{-3}$).
VED: Vitreous endosperm density ($g\ cm^{-3}$).
FED: Floury endosperm density ($g\ cm^{-3}$).
*: $P < 0.01$.
**: $P < 0.05$.
***: $P < 0.1$.

ROC curve classification results, V:F and EKD had the best classification accuracies (92% and 93%, respectively) when predicting milling quality. From the PCA bi-plot it was also evident that V:F and EKD, as well as VEV, were more strongly correlated with the good milling hybrids (good milling kernels lying closer to the respective variables on the plot).

## 4. Conclusions

A procedure was presented that can efficiently measure volumes and calculate densities from a large number of maize kernels scanned simultaneously by an X-ray μCT scanner. Regardless of the lower resolution (80 μm) scans (compared to single kernel scans at 13.4 μm resolution), good classification accuracies were still obtained. In particular, when using EKD a worthy classification accuracy of 93% was obtained, indicating that enough variation with respect to the density differences determined amongst kernels differing in milling quality was captured with the lower resolution scans. The lower resolution scans did, however, result in less accurate results (SEL = 0.037 g) compared to the higher resolution scans (0.010 g). The more easily obtained volume measurements ranged in classification accuracies of 77%–92%, also indicating good classification for V:F (92%). The lower resolution scans also allowed for sufficient segmentation and quantification of the respective volumes. Due to the ability to quantify material density it is likely that classification of maize kernels of intermediately levels of milling quality would be possible. A relationship between all the volume and density variables was indicated by the loadings of a PCA bi-plot, except that of FEV. This was confirmed with Spearman's rank correlation coefficients. The high-throughput and the relaxed resolution requirements (making lower cost systems a possibility), both contribute to the potential of X-ray μCT as a viable process control method.

## Acknowledgements

This work is based on research supported in part by the National Research Foundation of South Africa (Grant specific unique reference number (UID) 76641, 83974 and 88057). Gratitude goes to the staff of CAF including Stephan le Roux, Jarlen Beukes and Stacy-Lee Lewis for X-ray μCT assistance and analysis. The authors acknowledge Sasko, a division of Pioneer Foods (Pty) Ltd (Paarl, South Africa) for supplying the percentage chop values. Prof Martin Kidd from the Centre for Statistical Consultation, Stellenbosch University, is thanked for his contribution towards the statistical analysis performed in this study.

## References

Chiremba, C., Rooney, L.W., Taylor, J.R.N., 2011. Relationships between simple grain quality parameters for the estimation of sorghum and maize hardness in commercial hybrid cultivars. Cereal Chem. 88, 570–575.
De Carvalho, M.L.M., Van Aelst, A.C., Van Eck, J.W., Hoekstra, F.A., 1999. Pre-harvest stress cracks in maize (Zea mays L.) kernels as characterized by visual, X-ray and low temperature scanning electron microscopical analysis: effect on kernel quality. Seed Sci. Res. 9, 227–236.
Delcour, J., Hoseney, R.C., 2010. Principles of Cereal Science and Technology, third ed. AACC International Press, Minnesota, USA.
Dombrink-Kurtzman, M.A., 1994. Examination of opaque mutants of maize by reversed-phase high-performance liquid chromatography and scanning electron microscopy. J. Cereal Sci. 19, 57–64.
Dorsey-Redding, C., Hurburgh, C.R., Johnson, L.A., Fox, S.R., 1991. Relationships among maize quality factors. Cereal Chem. 68 (6), 602–605.
Du Plessis, A., Meincken, M., Seifert, T., 2013. Quantitative determination of density and mass of polymeric materials using microfocus computed tomography. J. Nondestruct. Eval. 32, 413–417.
Erasmus, C., Taylor, J.R.N., 2004. Optimising the determination of maize endosperm vitreousness by a rapid non-destructive image analysis technique. J. Sci. Food Agric. 84, 920–930.
Fox, G., Manley, M., 2009. Hardness methods for testing maize kernels. J. Agric. Food Chem. 57, 5647–5657.
Gaytán-Martínez, M., Figueroa-Cárdenas, J., Reyes-Vega, M., Rincón-Sánchez, F., Morales- Sánchez, E., 2006. Microstructure of starch granule related to kernel hardness in corn. Rev. Fitotec. Mex. 29, 135–139.
Guelpa, A., Bevilacqua, M., Marini, F., O'Kennedy, K., Geladi, P., Manley, M., 2015a. Application of Rapid Visco Analyser (RVA) viscograms and chemometrics for maize hardness characterisation. Food Chem. 173, 1220–1227.
Guelpa, A., Du Plessis, A., Kidd, M., Manley, M., 2015b. Non-destructive estimation of maize (*Zea mays* L.) kernel hardness by means of an X-ray micro-computed tomography (μCT) density calibration. Food Bioprocess Technol. 8, 1419–1429.
Gustin, J.L., Jackson, S., Williams, C., Patel, A., Armstrong, P.R., Peter, G.F., Settles, A.M., 2013. Analysis of maize (*Zea mays*) kernel density and volume using micro-computed tomography and single-kernel near infrared spectroscopy. J. Agric. Food Chem. 61, 10872–10880.
Lee, E., Young, J., Frégeau-Reid, J., Good, B., 2012. Genetic architecture underlying kernel quality in food-grade maize. Crop Sci. 52, 1561–1571.
Lee, K.M., Bean, S.R., Alavi, S., Herrman, T.J., Waniska, R.D., 2006. Physical and biochemical properties of maize hardness and extrudates of selected hybrids. J. Agric. Food Chem. 54, 4260–4269.
McGoverin, C., Manley, M., 2012. Classification of maize kernel hardness using near infrared hyperspectral imaging. J. Near Infrared Spectrosc. 20, 529–535.
Mestres, C., Louis-Alexandre, A., Matencio, F., Lahlou, A., 1991. Dry-milling properties of maize. Cereal Chem. 68, 51–56.
Paiva, E., Kriz, A.L., Peixoto, M.J.V.V.D., Wallace, J.C., Larkins, A.B., 1991. Quantitation and distribution of ā–zein in the endosperm of maize kernels. Cereal Chem. 68, 276–279.
Paulsen, M., Hill, L., 1985. Corn quality factors affecting dry milling performance. J. Agric. Eng. Res. 31, 255–263.
Pomeranz, Y., Martin, C.R., Traylor, D.D., Lai, F.S., 1984. Corn hardness determination. Cereal Chem. 61, 147–150.
Robutti, J.L., 1995. Maize kernel hardness estimation in breeding by near-infrared transmission analysis. Cereal Chem. 72, 632–636.
Robutti, J.L., Borras, F.S., Eyherabide, G.H., 1997. Zein compositions of mechanically separated coarse and fine portions of maize kernels. Cereal Chem. 74, 75–78.
Serna-Saldivar, S.O., 2010. Cereal Grains: Properties, Processing, and Nutritional Attributes. CRC Press Inc, London, UK.
Singhal, A., Grande, J.C., Zhou, Z., 2013. Micro/Nano CT for visualization of internal structures. Microsc. Today 21, 16–22.
Steffenrem, A., Kvaalen, H., Dalen, K.S., Høibø, O.A., 2014. A high-throughput X-ray-based method for measurements of relative wood density from unprepared increment cores from Picea abies. Scand. J. For. Res. 29, 506–514.
Takhar, P.S., Maier, D.E., Campanella, O.H., Chen, G., 2011. Hybrid mixture theory based moisture transport and stress development in corn kernels during drying: validation and simulation results. J. Food Eng. 106, 275–282.
Watson, S.A., 1987. Structure and composition. In: Watson, S.A., Ramstad, P.E. (Eds.), Corn Chemistry and Technology. American Association of Cereal Chemists, Inc., St. Paul, Minnesota, USA, pp. 53–82.
Weber, C., Dai Pra, A.L., Passoni, L.I., Rabal, H.J., Trivi, M., Poggio Aguerre, G.J., 2014. Determination of maize hardness by biospeckle and fuzzy granularity. Food Sci. Nutr. 2, 557–564.
Yang, W., Duan, L., Chen, G., Xiong, L., Liu, Q., 2013. Plant phenomics and high-throughput phenotyping: accelerating rice functional genomics using multidisciplinary technologies. Curr. Opin. plant Biol. 16, 180–187.
Yang, W., Xu, X., Duan, L., Luo, Q., Chen, S., Zeng, S., Liu, Q., 2011. High-throughput measurement of rice tillers using a conveyor equipped with X-ray computed tomography. Rev. Sci. Instrum. 82, 025102.